Wide Adoption of Grid-Forming Inverters and Their Impact on a Power Grid: A Case Study of the ERCOT Grid

Amro Quedan, Hamzeh Davarikia, Mehdi Daryabak, Yunzhi Cheng, Shun-Hsien (Fred) Huang

Abstract— **The power grid has been undergoing rapid and significant changes over the past two decades which the grid dynamic characteristic must be assessed regularly along with the integration of inverter-based resources (IBR). Similar to synchronous generator integration, control mechanisms such as automatic voltage control and power system stabilizers are adopted to facilitate coordination and ensure the stability of a power grid dominated by synchronous generators. With the significant growth of IBRs, ERCOT continuously assesses grid stability to ensure reliable operation. While multiple enhancements had been adopted, such as adding synchronous condensers, requiring IBRs provide voltage and frequency support and ride through performance, ERCOT has also established the Advanced Grid Support (AGS) requirements to new Energy Storage Resources to provide Grid-Forming (GFM) support that is necessary to maintain grid stability. While the implementation and penetration of AGS is not expected to occur immediately, this paper investigates the potential system wide adoption of Grid-forming Inverters (GFMIs) in the ERCOT grid for various IBRs considering their inherent existing operational limitations. Simulation results show that large-scale GFMIs deployment improves voltage and frequency responses following system contingencies, leveraging the ability of GFM IBRs to provide dynamic support across multiple time frames. Moreover, the small-signal stability assessment indicates that adoption of GFM control in the existing Battery Energy Storage System (BESS) can enhance the system's small-signal stability.**

Index Terms— **Grid-forming inverter, Inverter-based resources, Weak Grid.**

I. Introduction

The Electric Reliability Council of Texas (ERCOT) has installed capacities of 39.9 GW of wind, 32.7 GW of solar, and 14.1 GW of Battery Energy Storage system (BESS) as of July 2025 [1]. The highest ERCOT instantaneous penetration, defined as the instantaneous percentage of total system demand, from wind and solar together has reached 76%. Currently, these inverter-based resources (IBRs) are connected to the transmission grid using Grid-Following Inverters (GFLIs), which require certain level of grid strength to maintain stable operations. To support higher IBR penetration while maintaining system stability, solutions such as STATCOMs and synchronous condensers (SynCons) have been adopted. Model quality tests also help identify the GFL IBRs' capability to operate at various system strength levels, including weak grid conditions. More recently, Grid-Forming Inverters (GFMIs) have been proposed and adopted to require new BESS to provide advanced grid support.

Several studies in the literature have demonstrated the benefits of GFMIs deployment. In [2], a GFM BESS was evaluated alongside GFL wind and solar generation units, showing that the deployment of GFM BESS improves grid stability and reduced reliance on load-shedding schemes in Alaska's grid. Based on studies conducted by Hawaiian Electric, the deployment of a 30 MVA BESS on Maui Island significantly improved system damping, frequency nadir, and the rate of change of frequency (RoCoF) [3]. In the Australian Energy Market Operator (AEMO) grid, the Dalrymple GFM BESS demonstrated the capability to maintain grid stability and provide tight regulation of frequency and voltage following a disturbance [4]. Another study on the AEMO system demonstrated that configuring all operating BESS as GFMIs can enhance system voltage support [5]. In [6], the wide adoption of GFMIs was studied in Western Interconnection for up to 62%. The study showed the impact on inter-area oscillation modes, including their characteristics and observability. The results demonstrated that the wide adoption of GFMIs was able to damp a mode that affected system stability.

Prior to the adoption of Advanced Grid Support (AGS) requirements, ERCOT evaluated the potential impact of GFM through various studies including localized weak grids and broader West Texas region with more than 50 GW IBRs connected. The simulation results demonstrated that the GFM BESSs can improve the stability under weak grid conditions, transient grid voltage, thus potentially reducing the incidence of IBR trips [7] [8].

In this paper, a case study using both time domain and small signal stability analysis with the assumed wide adoption of GFM was conducted to help provide deeper insight into the dynamic performance and potential stability improvements associated with large-scale GFMIs deployment, while also identifying any potential area of concern that may arise to provide awareness and develop future plans if needed.

The rest of this paper is organized as follows: Section II describes the study scenarios. Section III presents the GFM models and assumptions. Section IV presents the simulation results. Finally, Section V concludes the paper and summarizes its contributions.

II. Case Condition description

A high-renewable, minimum-load base case scenario was selected to evaluate potential grid impact with a wide adoption of GFMIs on the transmission system under various study scenarios. The results are provided for illustrative purposes to support the findings and observations and do not represent actual grid impacts. Table I summarizes the online apparent power capacity (Sbase), active power dispatch (Pgen), and maximum active power (Pmax) of each resource type in the base case.

In the base case, all IBRs are assumed to be GFL IBRs to reflect existing grid conditions. Also, a large portion of installed IBRs (wind, solar, and energy) are located in the West Texas where the major load centers (such as Dallas, Houston, Austin, and

A. Quedan, H. Davarikia, M. Daryabak, Y. Cheng (yunzhi.cheng@ercot.com), and S. Huang are with the Electric Reliability Council of Texas (ERCOT), Taylor, TX, 76574

979-8-3315-8138-1

San Antonio) are in the central and coastal regions in Texas. Limited synchronous generators are located in West Texas and often not online when renewable generation is high. Therefore, the system strength in West Texas in this scenario could be reduced and lead to more volatile voltage responses.

Table I. Generation Types and Ratings

Type	Pgen (GW)	Pmax (GW)	Sbase (GVA)
SG	19.2	28.9	35.7
Solar	16.9	39.8	43.5
Wind	20.3	40.8	43.6
BESS	2.2	17.5	20.9

III. GFM MODEL

In this paper, a generic droop-based model (REGFM_A1) [9], originally developed to represent GFM BESS, is used to replace the original GFL model to all IBRs. To apply this model to solar and wind units, Pmax was set to Pgen (dispatched power), and Pmin was set to zero in this study that wind and solar units would not absorb active power (i.e., BESS charging mode) and restrict long-term active power response. This assumption is justified because the short-term dynamic response is primarily governed by the DC bus capacitors, which assumed to provide sufficient energy support for GFM operation. Furthermore, wind and solar units are typically operated under maximum power point tracking (MPPT), a condition adopted in this study without allocating headroom reserves. For clarity, the schematic of the model is shown in Figure 1.

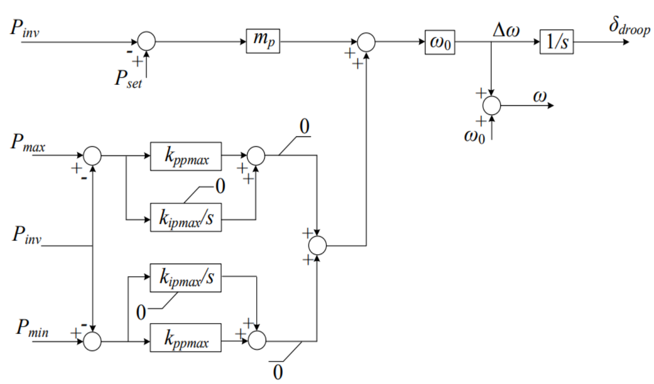

Figure 1. REGFM_A1 active power control model [9].

To investigate the active power response of both GFM BESS and GFM Solar/Wind, a Single Machine Infinite Bus (SMIB) system was used as shown in Figure 2. The size of the GFMI is 100MVA and the initial dispatch is 50%. At t = 5 s, a frequency step-down was added to the SMIB system from 60.0 Hz to 59.7 Hz. The corresponding active power response of GFM BESS and GFM Solar/Wind is shown in Figure 3. The GFM BESS demonstrated both short-term and long-term power response, resulting in a sustained increase in active power.

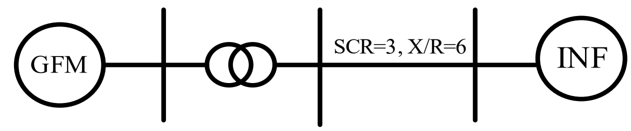

Figure 2. SMIB system schematic

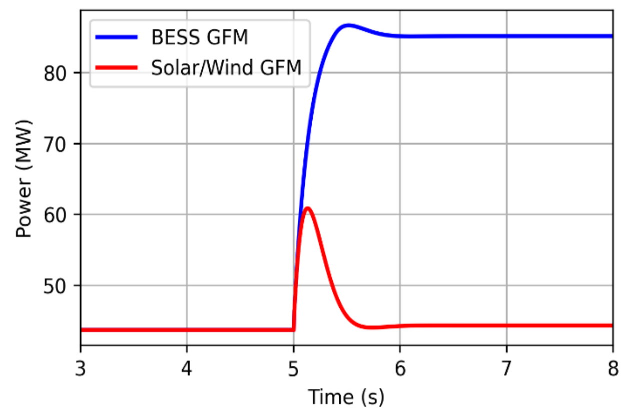

Figure 3. Active power response for GFM BESS and GFM Solar/Wind in SMIB test.

Parameters used in REGFM_A1 model for GFMIs are listed in Table II [9]. It is worth noting that both active power and reactive power droop gains were set to 1%, and maximum current capacity of inverters to 1.2 p.u. While each dynamic model representing an actual IBR would typically have configuration parameters specific to its design and location, the GFM model employed in this study represents all IBRs using identical settings.

Table II. BESS GFM REGFM_A1 parameters values

Parmeter	Value	Parameter	Value	Parameter	Value
mq	0.01	kipmax	0.1	TPf	0.01
kpv	0	Pmax	0.9	Imax	1.2
kiv	5.86	Pmin	-0.9	Qmax	0.44
mp	0.01	Emax	1.25	Qmin	-0.44
kppmax	0.01	Emin	0	kpqmax	0.1
kiqmax	20	TQf	0.01	TVf	0.01
		Vflag	0		

IV. SIMULATION RESULTS

A. Time-domain studies in positive sequence dynamic simulation

The validation of the REGFM_A1 positive-sequence model against the detailed electromagnetic transient (EMT) model confirms its consistency between the two models [10]. Consequently, all system-wide simulations presented in this paper are conducted in the positive-sequence domain, enabling comprehensive assessment of GFM behavior at the system level. Five scenarios representing different penetration of

979-8-3315-8138-1

GFMs in the grid were simulated using positive sequence time-domain simulations:

Case 1: All IBRs (solar, wind, and BESS) operate as GFL (base case).

Case 2: Apply generic GFM models to all Solar; Wind and BESS remain as GFL as in Case 1.

Case 3: Apply generic GFM models to all Wind; Solar and BESS remain as GFL as in Case 1.

Case 4: Apply generic GFM models to all BESS; Solar and Wind remain as GFL as in Case 1.

Case 5: Apply generic GFM models to all IBRs.

In all five cases, GFM performance was evaluated under a loss-of-generation contingency involving a total active power loss of 2.6 GW at t = 3 s, without a fault. Figure 4 -7 illustrate the total active power responses of solar, wind, BESS, and SGs for Case1 through Case 5. In addition, Figure 8 shows the total power output of all IBRs for the five cases above.

The solar output in all five cases are shown in Figure 4. As expected, there is no notable active power response from solar in Case 1, 3, and 4 when they are modeled as GFL with no additional headroom to respond to a frequency dip. GFM solar units provide an instantaneous active power increase following the SG trip in Case 2 and 5. In addition, the higher total solar active power response observed in Case 2 compared to Case 5 is attributed to the contribution of other GFMIs, such as those from wind and BESS units, providing frequency support in Case 5. Therefore, GFM Solar in Case 5 is not the sole resource type to respond to a frequency event. The additional frequency support from other IBRs decreases dependence on a single resource and reduces the effect of the event on the grid frequency.

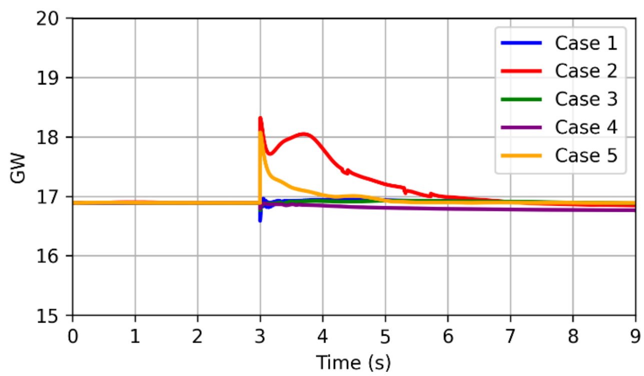

Figure 4. All Solar total active power output

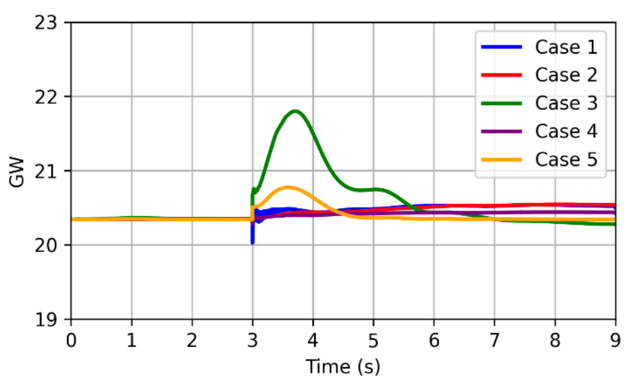

Figure 5. All Wind total active power output

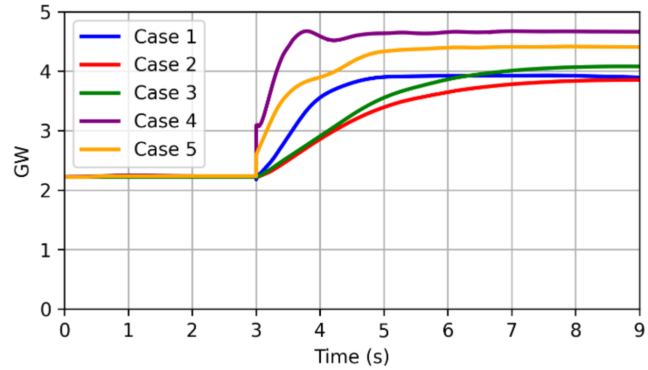

Figure 6. All BESSs total active power output

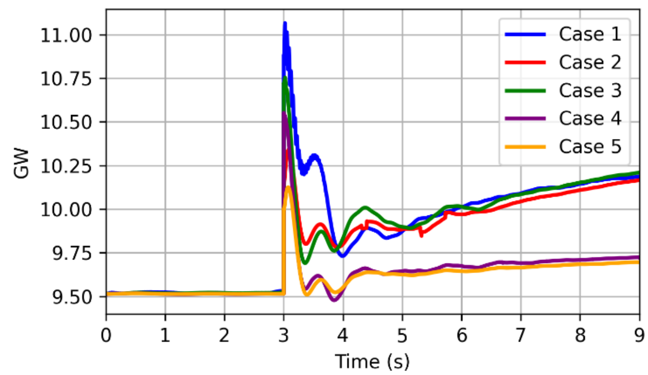

Figure 7. SGs total active power output

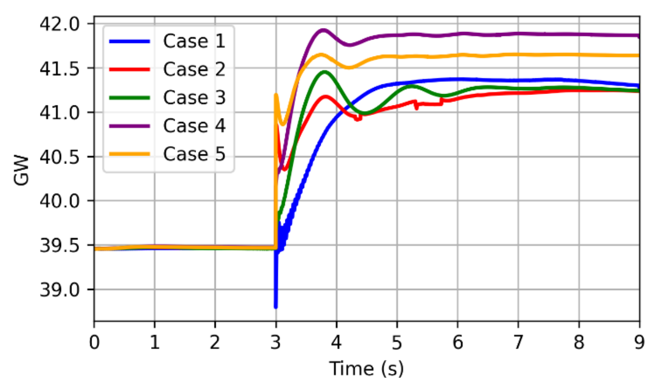

Figure 8. All IBR total active power output

A similar response is observed from the wind generation units in both Case 3 and Case 5, as shown in Figure 5. Nevertheless, this active power response is short-lived, even though the new frequency steady state value remains below the pre-disturbance value. Consequently, the active power eventually returns to its pre-disturbance level. This behavior was constrained in the dynamic model by setting Pmax=Pgen, as discussed in the previous section. The short-duration response is primarily supported by the energy stored in the DC bus capacitors. Again, it should be noted that the GFM model applied to both wind and solar in this study may not reflect the actual DC bus capacitor nor the energy buffer design but should still help to assess the impact on the grid. Further assessment will be conducted once the GFM wind and solar models and actual implementation are available.

BESS in all five cases are modeled to be capable of providing frequency support up to its Pmax and Pmin when operating at either charging or discharging modes, and its responses are shown in Figure 6. When the BESS generation units operate in GFM mode in Case 4 and 5, they provide both an instantaneous active power response and a sustained power increase governed by the frequency–power droop relationship. This is because these BESS units possess assumed headroom and stored energy to support the system frequency following the contingency.

The adoption of GFM operation in Cases 2–5 reduces the instantaneous active power response from the SGs, as shown in Figure 7. This reduction occurs because frequency support is shared between the SGs and the IBRs operating in GFM mode. The least instantaneous SG response occurs in Case 5, where all IBRs operate in GFM mode. This trend is consistent with Figure 8, which shows that the maximum instantaneous active power response from the IBRs is observed in Case 5.

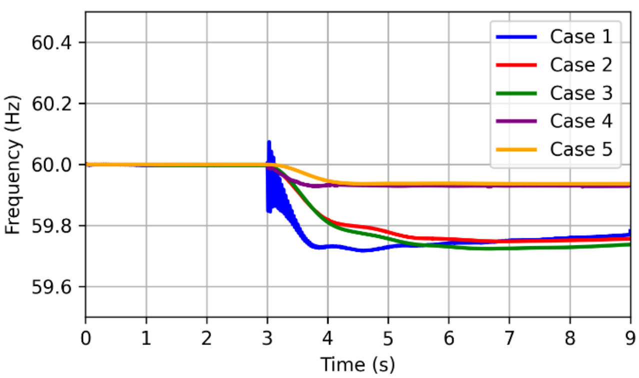

Figure 9. 345-kV bus frequency

With the adoption of GFM across the grid, it can be observed that GFM units enhance the frequency nadir, as shown in Figure 9. Among the generation units, BESSs provide effective response due to its contribution to both instantaneous and sustained active power responses with assumed headroom and state of charge. By contrast, solar and wind units are limited to providing only the inertia-like response based on the applied GFM model, assuming no headroom available and ideal DC capacity and energy buffer to provide instantaneous active power support.

Another key observation is that no major undesired response is observed in any of the tested cases, even under wide deployment of GFMIs using universal parameter settings. Although this may provide an indication that coordination challenges could be mitigated compared with existing weak grid challenges faced by the GFL IBRs, it must be noted that all new resources, including GFL and GFM IBRs, are required to go through the well-established interconnection process and studies to ensure all the resources can meet the grid codes and grid stability prior to actual operation. Additionally, monitoring and performance validation using adequate recording devices such as phasor measurement units and digital fault recorders are essential to ensure the new technology can be reliably integrated into the grid.

B. Small-signal studies based on positive-sequence model

In this section, the grid performance is evaluated in terms of small-signal stability in Case 1 and Case 4. In both cases, the same loss-of-generation contingency is applied. The resulting power flow cases, along with the corresponding dynamic data, are analyzed through small-signal stability and damping analysis. Figure 10 shows system modes (eigenvalues) for both cases, where the red points represent the modes for Case 1 and the blue points represent the modes for Case 4. It is worth noting that the ERCOT system includes dynamic data for SGs, IBRs, and reactive power control devices such as SVCs and STATCOMs. These modes represent the small-signal response of the system's dynamic elements for which SSAT supports the dynamic models.

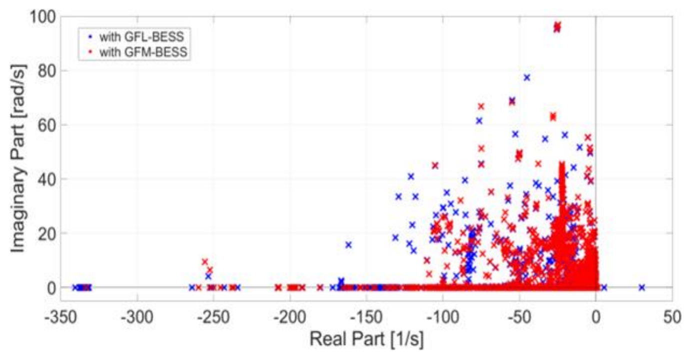

Figure 10. System modes with the BESS modeled as GFL (blue) and GFM (red).

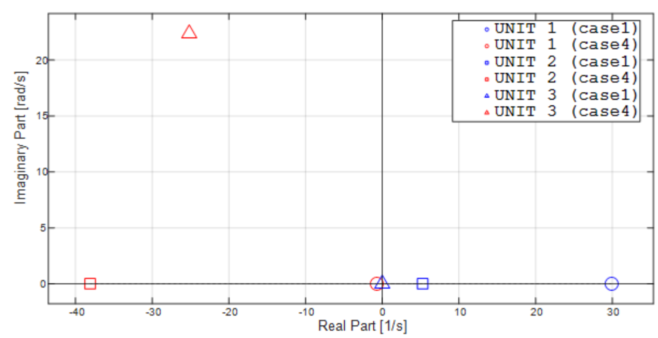

Figure 11. Displacement of three system modes with the BESS modeled as GFL (blue) versus GFM (red).

As observed, several modes in Case 1 appear in the right-half plane, which is expected given the stress imposed by the loss of generation event. In Case 4, three modes associated with non-BESS units shift further to the left, indicating increased damping and, consequently, enhanced system stability. The displacement of these modes is illustrated in Figure 11 that no modes are in the right-half plane which indicates the unstable response. These results demonstrate that GFM operation of BESS units could also enhance small-signal stability and reduce oscillation risks without introducing adverse modal interactions.

V. Conclusion

This paper investigates the application of GFM control as a viable solution to support grid stability. Three representative cases were developed, each examining a single energy resource configured to operate in GFM mode while incorporating the

979-8-3315-8138-1

resource's specific energy characteristics and operational constraints. In addition, a system-wide case was analyzed in which all IBRs across the ERCOT grid operated under GFM control. Both time-domain simulations and small-signal stability analyses were conducted to evaluate the performance of these developed cases. The results demonstrate that GFM control provides effective support for both voltage and frequency regulation, even under high-IBR penetration. Furthermore, the small-signal analysis revealed that GFM operation can beneficially displace system modes toward the left-half plane, indicating improved damping and overall system stability. No adverse interactions or instability were observed under large-scale GFM deployment.

In this study, the effect of PPC was not included due to software limitations in the model; however, PPC could influence system response and warrants future assessment. Additionally, only the droop-based generic model was considered for GFM control. Alternative control strategies for GFM, such as VSM or hybrid combinations, should be investigated in subsequent studies. Overall, these findings demonstrate that broad GFM deployment can enhance the dynamic resilience of the ERCOT grid. However, successful large-scale implementation will require proper model validation, coordinated parameter tuning, and alignment with interconnection requirements to ensure reliable grid operation under high IBR penetration.

VI. Acknowledgments

The authors would like to thank Dr. Wei Du from PNNL for his support with the GFM BESS PSS®E models, and Dr. Jeff Bloemink from PowerTech Labs for his assistance with the GFM TSAT and SSAT models.

VII. References

[1] The Electric Reliability Council of Texas (ERCOT), "Fact Sheet," July, 2025.

[2] M. Richwine, I. Anselmo, P. Cicilio and A. Francisco, "Grid-Forming Inverter Batteries for Enhanced System Stability in Alaska's Islanded Railbelt Electric Grid," in *IEEE Power & Energy Society General Meeting (PESGM)*, Seattle, WA, USA,, 2024.

[3] A. Hoke, W. Kenyon, B. Wang, J. Tan, G. Yau, M. Asano and L. Dangelmaier, "Inverter-Based Operation of Maui: Electromagnetic Transient Simulations.," in *No. NREL/PR-5D00-79852, National Renewable Energy Lab.(NREL),*, Golden, CO (United States), 2021.

[4] Australian Energy Market Operator (AEMO), "Analysis and modelling of a gridforming battery energy storage system during a system incident," 2024.

[5] Transgrid, "Meeting system strength requirements in NSW," 2025.

[6] PACIFIC NORTHWEST NATIONAL LABORATORY (PNNL), "How a Large-Scale Deployment of Grid-Forming Inverters May Impact Inter--Area Oscillation. Modes An Investigation in the US," 2023.

[7] A. Quedan, A. Goharrizi, Y. Cheng, S.-H. F. Huang, W. Du and D. Ramasubramanian., "Grid-Forming Inverters for Stability Improvements in Bulk Power Systems with High Inverter-Based Resources Penetration," in *2024 IEEE Power & Energy Society General Meeting (PESGM)*, Seattle, WA, USA, 2024.

[8] A. Quedan, A. Goharrizi, Y. Cheng and S.-H. F. Huang, "Weak grid test case development and enhancement for high penetration of inverter-based resources," in *2024 IEEE Power & Energy Society General Meeting (PESGM)*, Seattle, WA, USA, 2024.

[9] W. Du, "Model Specification of Droop-Controlled, GridForming Inverters (REGFM_A1)," No.PNNL - 35110. Pacific Northwest National Laboratory (PNNL), Richland, WA (United States), 2023.

[10] W. Du et al., "Positive-Sequence Modeling of Droop-Controlled Grid-Forming Inverters for Transient Stability Simulation of Transmission Systems," *IEEE Transactions on Power Delivery,* vol. 39, no. 3, pp. 1736-1748, June 2024.